Polyhedron 231 (2023) 116272

Contents lists available at ScienceDirect

Polyhedron

journal homepage: www.elsevier.com/locate/poly

Synthesis, structural and spectral characteristics of novel n,π-chelate complexes of Pd(II) and Pt(II) with *N*-allylthioureas and their influence on the growth of spheroids cells MCF-7 and GGT activity

Svitlana I. Orysyk [a,*], Yurii L. Zborovskii [b], Viktor V. Orysyk [b], Liudmyla V. Garmanchuk [c], Polina V. Borovyk [a], Svitlana V. Shishkina [d], Olha Pavliuk [e], Vasyl I. Pekhnyo [a], Mykhailo V. Vovk [b]

[a] *V.I. Vernadsky Institute of General and Inorganic Chemistry NAS of Ukraine, Palladin Ave. 32/34, 03147 Kyiv, Ukraine*
[b] *Institute of Organic Chemistry, NAS of Ukraine, Murmanska Str. 5, 02660 Kyiv, Ukraine*
[c] *Taras Shevchencko National University, Educational and Scientific Centre "Institute of Biology", Glushkov Ave. 2, 03022 Kyiv, Ukraine*
[d] *SSI "Institute for Single Crystals", National Academy of Science of Ukraine, 60 Nauky Ave., Kharkiv 61001, Ukraine*
[e] *National University of Life and Environmental Sciences of Ukraine, Heroyiv Oborony St., 15, Kyiv 03041, Ukraine*

ARTICLE INFO

Keywords:
Pd(II)/Pt(II) π-complexes
X-ray diffraction study
IR
UV–vis
NMR spectra
Anti-metastatic
Pro-apoptotic effect
MCF-7 cell spheroids
GGT activity
Bioinorganic chemistry
Antitumor agents
X-ray study

ABSTRACT

Four mononuclear n,π-chelate complexes $[M(HL^{1,2})Cl_2]$ ($M = Pd^{2+}$, Pt^{2+}) have been obtained by the reactions of $PdCl_2$ or $K_2[PtCl_4]$ with *N*,*N*-diethyl-*N'*-(2-propenyl)thiourea (HL^1) or *N*-cyclohexyl-*N'*-(2-propenyl)thiourea (HL^2) in the presence of HCl. According to X-ray diffraction study, the molecules of $HL^{1,2}$ are coordinated in a bidentate manner with the formation of six-membered chelate metallocycles in a twist-boat conformation. The diagonal arrangement of "soft-hard" donor atoms (S–M–Cl, C–M–Cl) in the coordination sphere leads to the Pearson's effect of "molecular antisymbiosis in the *trans* effect" that causes the formation of complexes with an M:L ratio of 1:1. However, interaction in the ratio 1:2, 1:3 is also possible in the solution under the conditions of monodentate coordination of HL^1 and HL^2. All compounds were investigated by IR, UV–vis and NMR spectra. The $^1H/^{13}C$ NMR study showed that this method is reliable for establishing the formation of a π-coordinating bond. The similarity of the synthesized complexes structure with cisplatin implies the same mechanism of their antitumor action. Thus, it was investigated their effect on the growth and biochemical characteristics of human breast adenocarcinoma cells MCF-7 (grown in three-dimensional culture as spheroids) and the activity of the enzyme gamma-glutamyl transpeptidase (GGT). The results showed that all studied π-complexes are more active compared to cisplatin, and they exhibit pronounced *anti*-metastatic and *pro*-apoptotic activity, which one is caused by their inhibitory effect.

1. Introduction

Alkyl-, aryl-, and heteroaryl-substituted thioureas are an important class of organic compounds that are used as building blocks for the generation of N- and S-containing heterocycles [1–4]. The ability of polyfunctional thioureas to effect non-covalent interaction with functional groups H-bond acceptors (C═O, NH_2, *N*-containing heterocycls, etc. [5]) allows them to interact with peptide and heterocyclic moieties of enzymes, proteins, cellular receptors, nucleic acids and other drug molecular targets, which determines their high anticancer [6,7], antiviral [8,9], antibacterial [10–12], antifungal [13,14], antiangiogenic activity [15], etc. Therefore, they are one of the most widely used scaffolds in medicinal chemistry [16,17].

In coordination chemistry, *N*-substituted derivatives of thiourea are versatile reagents capable of coordinating the ions of many metals. The presence of N,S-donor atoms of thioureide group allows them to coordinate to metal ions in monodentate manner (only through the sulfur [18–21]), or bidentate N,S-chelating mode with the formation of a four-membered metallocycles [22–25]. Depending on the solvent properties and pH reaction media, thioureas can coordinate to metal ions as neutral, monoanionic or dianionic ligands [26–28]. However, the combination of the thioureide group with other "hard" and "soft" donor

* Corresponding author.
E-mail address: s.oryslend@gmail.com (S.I. Orysyk).

https://doi.org/10.1016/j.poly.2022.116272
Received 13 September 2022; Accepted 20 December 2022
Available online 23 December 2022

atoms in substituted moieties enable polyfunctional thioureas to react readily with transition metal ions, forming stable five- and six-membered chelate metallocycles [29–36]. This property allows them to be used as analytical reagents for the qualitative and quantitative determination of metals in natural or technological objects [37–39]. At the same time, chelate type complexes are characterized by good metabolic stability, since the coordination of ligands in them largely inhibits hydrolysis of salts in biological media. Moreover, complexation promotes the penetration of metal ions through cell membranes. Therefore, they are valuable objects of bioinorganic chemistry. This is especially true for compounds of platinum group metals [40,41]. In addition, substituted thioureas have a number of advantages: they are low-toxic, and the methods of their synthesis and modification are simple.

Previously, we installed that *N*-allylthiourea derivatives are effective chelating agents due to the favorable spatial location of the allylic moiety in them relative to the S-nucleophilic reaction center, which creates prerequisites for the formation of stable six-membered chelate metallocycles with the generation of π-bonds with such "soft" Lewis acids as Pd(II), Pt(II) and Ag(I) [42–44]. At the same time, our previous studies showed that *N*-allyl-substituted thioureas form a π-bond under conditions when other donor atoms are in an unfavorable position for the formation of a chelate metallocycle. Otherwise, the «soft» Lewis acids will be coordinated to other donor centers [45–47]. Therefore, in the *N,N*-diethyl-*N'*-(2-propenyl)thiourea (HL^1) and *N*-cyclohexyl-*N'*-(2-propenyl)thiourea (HL^2) used in this work, the spatial arrangement of the N,S-nucleophilic centers to the allylic moiety is also favorable for the formation of the n,π-chelate metallocycle. Among the series of previously synthesized compounds, a number of Pt(II) and Pd(II) mononuclear π-coordination complexes showed a high affinity to DNA with cytostatic and proapoptotic effects which was superior to that of cisplatin [42,44,48]. We proceeded from the assumption that such compounds may have the prospect of overcoming the resistance of pathogenic cells to their action due to the coordination of *N*-allyl-substituted thiourea. It is known that one of the ways to overcome the resistance inherent in cisplatin is to prevent its binding to thiol-containing compounds (such as the tripeptide glutathione, metallothioneins, or other proteins rich in sulfur-containing amino acids: cysteine and methionine) located in the blood cytoplasm because, as a result of interaction with ones, the antitumor agent loses the DNA-binding ability. Unlike cisplatin and its analogues, *N*-allylthioureas are coordinated by even "softer" sulfur and carbon atoms in synthesized π-complexes, which should prevent the interaction of central atoms with thiol-containing compounds because of the Pearson's effect of "molecular antisymbiosis in the *trans* effect" begins to operate [49]. In order to test this assumption, the novel Pd(II) and Pt(II) n,π-chelate complexes with alkyl-thioureas HL^1 and HL^2 were obtained. Also, we tried to indirectly prove the ability of such compounds to overcome the resistance of pathogenic cells, using the example of studying their effect on the growth of multicellular spheroids of MCF-7 breast tumor cells and the activity of the enzyme gamma-glutamyl transpeptidase (GGT), which is the main target of action of cisplatin and its structural analogs.

2. Experimental section

2.1. Materials and methods

Initial reagents ($PdCl_2$, $K_2[PtCl_4]$) and solvents (ethanol, hydrochloric acid, and diethyl ether) used in this work were of synthetic grade and used as purchased without further purification. Elemental analyses for carbon, hydrogen, nitrogen and sulfur were performed by Carlo Erba Elemental Analyzer (Model 1106). The chlorine was measured by the Schoniger method. $^1H/^{13}C$ NMR spectra were measured on a Bruker Avance DRX-400 (or DRX-500) spectrometer (400.00, 500.00/125.75 MHz) in DMSO-d_6 solution using tetramethylsilane (TMS) as internal standard (Fig. S1–S6). All assignments are based on literary data [50,51] and theoretical predict of $^1H/^{13}C$ NMR shifts according to the program ChemBioDraw Uitra 12. Attenuated total internal reflection Fourier transform infrared (ATR-FT-IR) spectra were recorded on a Thermo Nicolet Nexus 4700 FT-IR spectrometer in a range of 4000–400 cm^{-1} (Fig S7). The assignment of the bands was performed earlier at BP86/MCP-TZP level of theory at [48] and compared with data in [51–54]. Solid state reflectance spectra and UV–vis spectra of ethanol-DMF (2:1) solutions of ligand and complexes were measured on a Specord M40 in a range of 200–1000 nm^{-1}. The assignment of absorption bands was performed according to the data in [51,55,56].

The studies of complex formation in ethanol solution were performed using spectrophotometric titration [48]. The starting solutions for titration were prepared by dissolving an exact mass of $PdCl_2$ (or $K_2[PtCl_4]$ in 4 ml of 2 M HCl, and the thioureas HL^1, HL^2 in EtOH and brought to a volume of 25 ml with ethanol. Herewith the concentration of metal salts (C_M) was unchanged (10×10^{-5} M), while the concentration of thioureas HL^1 and HL^2 was changed from 1.67×10^{-5} M to 33.33×10^{-5} M (Fig. S8).

2.2. Preparation of thioureas HL^1, HL^2 and complexes I–IV

N,N-Diethyl-*N'*-(2-propenyl)thiourea (HL^1) and *N*-cyclohexyl-*N'*-(2-propenyl)thiourea (HL^2) were obtained by reacting allyl isothiocyanate with diethylamine or cyclohexylamine in accordance with the methods [57,58]. Previously, HL^2 was obtained by a similar method and was used as an intermediate synthon without isolation from the reaction mixture for the preparation of 1-allyl-3-cyclohexyl-2-methylisothiourea hydroiodide [58]. Both allylthioureas have not previously been used in coordination chemistry as ligands for metal complexes.

HL^1, Calculated for $C_8H_{16}N_2S$: C, 55.77; H, 9.36; N, 16.26; S, 18.61%. Found: C, 55.70; H, 9.41; N, 16.12; S, 18.45%. NMR ^1H, (*δ*, ppm): 7.45 m (1H, N^1H); 5.87 m (1H, $-C^2H=$); 5.08 d (1H, $=C^1H_{trans}$, *J* 17.0 Hz); 5.04 d (1H, $=C^1H_{cis}$, *J* 10.5 Hz); 4.14 br.m (2H, C^3H_2); 3.62 dd (4H, $C^5H_2 + C^8H_2$, *J* 7 Hz, *J* 14 Hz); 1.08 t (6H, $C^6H_3 + C^7H_3$, *J* 7 Hz). NMR ^{13}C, (*δ*, ppm): 180.05 C^4, 136.46 C^2, 115.26 C^1, 47.92 C^3, 44.68 $C^{5,8}$, 13.16 $C^{6,7}$. IR (*ν*, cm^{-1}): 3300 *ν*(NH); 3090 $\nu_{as}(CH)_{allyl}$, 3060 $\nu_s(CH)_{allyl}$; 2990, 2955 $\nu_{as}(CH)_{CH3}$; 2917, 2870 $\nu_s(CH)_{CH3}$; 1535, 1500 δ(NH) + ν_{as}(NCN); 1439, 1403; ν_s(*N*-CS-N) + δ(CH); 1370–1320 $\delta_s(CH)_{CH3}$; 1275–1208 $\delta(CH)_{CH2}$; 1032 *ν*(C═S); 920 $\delta(CH)_{-C=CH}$. UV–vis, (λ, nm (log ε)): 290 (2.71).

HL^2, Calculated for $C_{10}H_{18}N_2S$: C, 60.56; H, 9.15; N, 14.12; S, 16.17%. Found: C, 60.45; H, 9.18; N, 14.00; S, 16.08%. NMR ^1H, (*δ*, ppm): 7.33 m (1H, N^1H); 7.28 m (1H, N^2H); 5.84 m (1H, $-C^2H=$); 5.14 d (1H, $=C^1H_{trans}$, *J* 15.5 Hz); 5.07 d (1H, $=C^1H_{cis}$, *J* 10.5 Hz); 4.04 br.m (2H, C^3H_2); 2.53 m (1H, $C^5H_{cyclohexyl}$); 1.84 m (2H, $CH_{cyclohexyl}$); 1.65 m (2H, $CH_{cyclohexyl}$); 1.54 m (1H, $CH_{cyclohexyl}$); 1.27 m (2H, $CH_{cyclohexyl}$); 1.16 m (3H, $CH_{cyclohexyl}$). NMR ^{13}C, (*δ*, ppm): 181.43 C^4, 135.72 C^2, 115.79 C^1, 52.21 C^5, 46.24 C^3, 32.74 $C^{6,10}$, 25.64 C^8, 24.97 $C^{7,9}$. IR, (*ν*, cm^{-1}): 3273, 3214 *ν*(NH); 3088 $\nu as(CH)_{allyl}$, 3018 $\nu_s(CH)_{allyl}$; 2935 $\nu as(CH)_{CH2}$, 2854 $\nu s(CH)_{CH2}$; 1567, 1519 δ(NH) + ν_{as}(NCN); 1447, 1405 ν_s(*N*-CS-N) + δ(CH); 1337–1234 $\delta(CH)_{CH2}$; 1110 *ν*(C═S); 911 $\delta(CH)_{-C=CH}$. UV–vis, (λ, nm(log ε)): 284 (2.72).

$[Pd(HL^{1,2})Cl_2]$ (**I, III**): $PdCl_2$ (88.7 mg, 0.5 mmol) was dissolved in 2 ml of 2 N HCl and 8 ml of ethanol with constant stirring and heating to 45 °C. The hot solution of thiourea HL^1 (86.1 mg) or HL^2 (99.2 mg, 0.5 mmol in 10 ml of ethanol) was slowly added to the resulting solution at constant stirring. The transparent solution of the mixture was heated (at 45 °C) for 15 min and left in a dark place. After four days, the light-brown plate crystals began to stand out which were filtered on the next day, washed with ethanol and diethyl ether.

$[Pd(HL^1)Cl_2]$ (**I**), Yield: 128 mg (73%). Calculated for $C_8H_{16}Cl_2N_2PdS$, %: C, 27.48; H, 4.61; Cl, 20.28; N, 8.01; S, 9.17. Found, %: C, 27.30; H, 4.70; Cl, 20.10; N, 7.85; S, 9.00. NMR ^1H, (*δ*, ppm): 8.73 m (1H, N^1H); 6.18 m (1H, $-C^2H=$); 4.40 d (1H, $=C^1H_{trans}$, *J* 14.5 Hz); 4.91 d (1H, $=C^1H_{cis}$, *J* 9.5 Hz); 4.21 d (1H, *J* 22.5 Hz, C^3H_2); 3.97 d (1H, *J* 22.0 Hz, C^3H_2); 3.54 dd, (4H, $C^5H_2 + C^8H_2$, *J* 8.5 Hz, *J* 18.0 Hz); 1.15 t (6H, $C^6H_3 + C^7H_3$, *J* 8.5 Hz). NMR ^{13}C, (*δ*, ppm): 170.37 C^4, 103.07 C^2,

77.41 C^1, 46.52 C^3, 40.06 $C^{5,8}$, 12.94 $C^{6,7}$. IR, (ν, cm^{-1}): 3320 ν(NH); 3120 νas$(CH)_{allyl}$, 3095 $\nu_s(CH)_{allyl}$; 2983, 2934 $\nu_{as}(CH)_{CH3}$; 2901, 2873 $\nu_s(CH)_{CH3}$; 1562, 1495 δ(NH) + ν_{as}(NCN); 1420, 1392 ν_s(*N*-CS-N) + δ(CH); 1380–1330 $\delta_s(CH)_{CH3}$; 1289–1201 $\delta(CH)_{CH2}$; 985 ν(C═S); 885 $\delta(CH)_{\text{-C=CH}}$. UV–vis, (λ, nm (log ε)): 327 (3.11); 370 (2.86); 465 (2.16).

$[Pd(HL^2)Cl_2]\cdot H_2O$ (**III**), Yield: 154 mg (82%). Calculated for $C_{10}H_{20}Cl_2N_2OPdS$, %: C, 30.51; H, 5.12; Cl, 18.01; N, 7.12; S, 8.15. Found, %: C, 30.35; H, 5.15; Cl, 18.10; N, 7.05; S, 8.00. NMR ^{1}H, (δ, ppm): 9.27 m (1H, N^1H); 9.01 m (1H, N^2H); 6.15 m (1H, $-C^2H=$); 4.36 d (1H, $=C^1H_{trans}$, *J* 14.0 Hz); 4.95 d (1H, $=C^1H_{cis}$, *J* 8.4 Hz); 4.19 d (1H, C^3H_2, *J* 17.6 Hz); 3.93 d (1H, C^3H_2, *J* 18.4 Hz); 3.46 m (1H, $C^5H_{cyclohexyl}$); 1.87 m (1H, $CH_{cyclohexyl}$); 1.70 m (2H, $CH_{cyclohexyl}$); 1.57 m (1H, $CH_{cyclohexyl}$); 1.24 m (5H, $CH_{cyclohexyl}$); 1.10 m (1H, $CH_{cyclohexyl}$). NMR ^{13}C, (δ, ppm): 169.37 C^4, 103.16 C^2, 77.76 C^1, 52.67 C^5, 45.93 C^3, 32.24 $C^{6,10}$, 25.15 C^8, 24.85 $C^{7,9}$. IR, (ν, cm^{-1}): 3530, 3475 $\nu(O—H)_{H2O}$; 3253 br. ν(NH); 3143 νas$(CH)_{allyl}$, 3026 $\nu_s(CH)_{allyl}$; 2930 νas$(CH)_{CH2}$, 2854 νs$(CH)_{CH2}$; 1595, 1533 δ(NH) + ν_{as}(NCN); 1450, 1395 ν_s(*N*-CS-N) + δ(CH); 1345–1227 $\delta(CH)_{CH2}$; 1066 ν(C═S); 887 $\delta(CH)_{\text{-C=CH}}$. UV–vis, (λ, nm (log ε)): 365 (3.30); 470 (2.68).

$[Pt(HL^{1,2})Cl_2]$ (**II**, **IV**): K_2PtCl_4 (207.5 mg, 0.5 mmol) was dissolved in 8 ml of distilled water. The resulting solution was acidified with 2 ml of 2 N HCl and heated to 45 °C. A hot solution of thiourea HL^1 (86.1 mg) or HL^2 (99.2 mg, 0.5 mmol in 10 ml of ethanol) was slowly added with constant stirring and heating. The transparent solution of the mixture was heated (at 55 °C) for 20 min and left in a dark place. After three days, yellow crystals began to stand out, which were filtered the next day, washed with ethanol and diethyl ether.

$[Pt(HL^1)Cl_2]\cdot$(**II**), Yield: 258 mg (88%). Calculated for $C_8H_{16}Cl_2N_2PtS$, %: C, 21.92; H, 3.68; Cl, 16.18; N, 6.39; S, 7.32. Found, %: C, 21.78; H, 3.70; Cl, 16.05; N, 6.25; S, 7.20. NMR ^{1}H, (δ, ppm): 8.75 m (1H, N^1H); 5.06 m (1H, $-C^2H=$); 3.67 d (1H, $=C^1H_{trans}$, *J* 12.8 Hz); 4.06 d (1H, $=C^1H_{cis}$, *J* 7.2 Hz); 4.28 d (1H, *J* 17.2 Hz, C^3H_2); 4.00 d (1H, *J* 15.6 Hz, C^3H_2); 3.51 dd, (4H, $C^5H_2 + C^8H_2$, *J* 7.2 Hz, *J* 14.0 Hz); 1.15 t (6H, $C^6H_3 + C^7H_3$, *J* 8.5 Hz). NMR ^{13}C, (δ, ppm): 166.92 C^4, 80.14 C^2, 58.85 C^1, 46.24 C^3, 40.21 $C^{5,8}$, 12.97 $C^{6,7}$. IR, (ν, cm^{-1}): 3330 ν(NH); 3130 νas$(CH)_{allyl}$, 3075 $\nu_s(CH)_{allyl}$; 2980, 2935 $\nu_{as}(CH)_{CH3}$; 2985, 2860 $\nu_s(CH)_{CH3}$; 1565, 1480 δ(NH) + ν_{as}(NCN); 1422, 1390 ν_s(*N*-CS-N) + δ(CH); 1356–1330 $\delta_s(CH)_{CH3}$; 1285–1200 $\delta(CH)_{CH2}$; 990 ν(C═S); 891 $\delta(CH)_{\text{-C=CH}}$. UV–vis, (λ, nm (log ε)): 307 (3.16); 389 (2.25); 400 (2.24).

$[Pt(HL^2)Cl_2]\cdot H_2O$ (**IV**), Yield: 245 mg (80%). Calculated for $C_{10}H_{20}Cl_2N_2OPtS$, %: C, 24.90; H, 4.18; Cl, 14.70; N, 5.81; S, 6.65. Found, %: C, 24.70; H, 4.20; Cl, 14.62; N, 5.80; S, 6.58. NMR ^{1}H, (δ, ppm): 9.16 m (1H, N^1H); 9.03 m (1H, N^2H); 5.03 m (1H, $-C^2H=$); 3.63 d (1H, $=C^1H_{trans}$, *J* 12.8 Hz); 4.08 d (1H, $=C^1H_{cis}$, *J* 7.6 Hz); 4.27 d (1H, C^3H_2, *J* 16.8 Hz); 3.95 d (1H, C^3H_2, *J* 15.6 Hz); 3.44 m (1H, $C^5H_{cyclohexyl}$); 1.86 m (1H, $CH_{cyclohexyl}$); 1.69 m (2H, $CH_{cyclohexyl}$); 1.57 m (1H, $CH_{cyclohexyl}$); 1.22 m (5H, $CH_{cyclohexyl}$); 1.09 m (1H, $CH_{cyclohexyl}$). NMR ^{13}C, (δ, ppm): 165.28 C^4, 79.48 C^2, 63.97 C^1, 52.46 C^5, 45.15 C^3, 32.26 $C^{6,10}$, 25.15 C^8, 24.86 $C^{7,9}$. IR, (ν, cm^{-1}): 3560, 3502 $\nu(O—H)_{H2O}$; 3280 br. ν(NH); 3150 νas$(CH)_{allyl}$, 3026 $\nu_s(CH)_{allyl}$; 2932 $\nu_{as}(CH)_{CH2}$, 2854 $\nu_s(CH)_{CH2}$; 1585, 1525 δ(NH) + ν_{as}(NCN); 1450, 1393 ν_s(*N*-CS-N) + δ(CH); 1345–1217 $\delta(CH)_{CH2}$; 1070 ν(C═S); 887 $\delta(CH)_{\text{-C=CH}}$. UV–vis, (λ, nm (log ε)): 305 (3.31); 385 (2.34); 397 (2.33).

2.3. Single crystal X-ray diffraction (SCXRD)

X-ray diffraction studies were performed on an automatic "Bruker APEX II" diffractometer (graphite monochromated MoKα radiation, CCD-detector, φ- and ω-scanning). The structures were solved by direct method using SHELXTL package [59]. Positions of the hydrogen atoms were located from electron density difference maps and refined by "riding" model with $U_{iso} = nU_{eq}$ of the carrier atom (n = 1.5 for water molecule and n = 1.2 for other hydrogen atoms). The hydrogen atoms of the allyl moiety coordinated to the metal atom were refined using isotropic approximation. The crystallographic data and experimental parameters are listed in Table 1. Final atomic coordinates, geometrical parameters and crystallographic data have been deposited with the Cambridge Crystallographic Data Centre, 11 Union Road, Cambridge, CB2 1EZ, UK (fax: +44 1223 336033; e-mail: deposit@ccdc.cam.ac.uk). The deposition numbers are given in Table 1.

Table 1
Data collection details and selected crystallographic data for complexes **III**, **IV**.

Compound	(III)	(IV)
Formula	$C_{10}H_{18}N_2SPdCl_2\cdot H_2O$	$C_{10}H_{18}N_2SPtCl_2\cdot H_2O$
Fw (g/mol)	393.64	482.32
Crystal system, Space group	Triclinic, P^1	
a (Å)	7.8512(10)	*7.759(3)*
b (Å)	8.4477(10)	8.470(3)
c (Å)	12.3343(16)	12.412(5)
α (°)	96.021(8)	97.412(13)
β (°)	107.009(7)	107.656(8)
γ (°)	102.048(7)	101.728(6)
V (Å^3)	752.91(17)	745.0(5)
Z	2	
ρ_{calc}/g·cm^{-3}	1.736	2.150
μ (mm^{-1})	1.713	9.903
R_1 [$I > 2\sigma(I)$][1]	0.0663	0.0295
R_1 (all data)[1]	0.0938	0.0368
wR_2 [$I > 2\sigma(I)$][1]	0.1703	0.0600
wR_2 [all data][1]	0.1824	0.0626
S	1.092	0.997
$\Delta\rho_{max,min}$ (e^-/A^3)	1.36, −1.27	1.67, −1.63
CCDC	2204095	2204096

[1] $R_1 = \sum||F_o| - |F_c||/\sum|F_o|$; $wR_2 = [\sum[w\,(F_o^2 - F_c^2)^2]/\sum[w(F_o^2)^2]]^{1/2}$, where $w = 1/[\sigma^2F_o^2 + (A\cdot P)^2 + (B\cdot P)]$, and $P = (F_o^2 + 2F_c^2)/3$; *A*, *B* are the respective weight coefficients.

2.4. Experimental methods used in biological research

2.4.1. Obtaining multicellular microspheroids

Generation of the spheroids cells MCF-7 was carried out as described by us earlier using carboxymethyl cellulose [60,61]. Cells in 3D culture were incubated during 7 days under conditions of starvation at 37 °C, 100% of humidity, 5% of CO_2 in Dulbecco's Modified Eagle Medium (DMEM) with the addition of 10% fetal bovine serum (FBS), 2 mmol L-glutamine, and 40 μg/ml gentamicin. Spheroids were generated using carboxymethylcellulose (0.2%). The investigated complexes were added to the culture of spheroids in concentrations 5 times lower than the determined IC50 indicator during cytotoxic screening of the complexes on cervical cancer cells line Hela (complex **I** – 3×10^{-5} M; complex **II** – 2×10^{-6} M; complex **III** – 4×10^{-7} M; complex **IV** – 5×10^{-6} M, respectively) [42]. The medium incubation was not changed during the long-term culturing. The sizes of the spheroids were determined using an inverted microscope Axiovert 40 with software Axio Vision. To do this, photographs (were taken in 20 fields of view and the dimensions of the spheroids were calculated, and their percentage ratio was determined in different ranges.

2.4.2. Determination of adhesive properties of cells

To evaluate adhesive properties of MCF-7 cells under the influence of studied compounds, the method of measuring adhesive abilities of macrophages was adapted. After incubation of cells with tested compounds, the culture medium was removed, and the layer of adherent cells was washed thrice with normal saline solution (pH 7.4). The cells were fixed for 30 min with addition of 100 μL 96% ethanol in each well. After fixation, ethanol was removed and the plate was thoroughly dried. The staining solution (crystal violet) was added to the fixed cells, 100 μL per well, and incubated for 15 min at 20 °C. After incubation, the staining solution was removed and the cells were thrice washed with normal saline solution. To the layer of stained cells, dimethyl sulfoxide was added per each well 100 μL and incubated for 15 min at 37 °C. After full dissolution of the stain, the optic density (OD) of solution was determined in each well using the spectrophotometer at 570 nm. The

results were given in adhesion index (AI) units, calculated as follows:

$$AI = E_e/E_c \cdot 100\% \ [\%],$$

(E_e is extinction of fluid, measured in the presence of studied compound; E_c is extinction of fluid in control wells).

2.4.3. Determination of γ-glutamyltransferase activity (GGT)

GGT in the culture medium of cells was determined using the standard kit (Filicit-Diagnostics, Ukraine). The principle of the method is that under the action of GGT, the glutamine residue from γ-L(+)-glutamyl-4-nitroanilide is transferred to a dipeptide acceptor glycylglycine. At the same time, a chromogen is released – *p*-nitroaniline, the concentration of which is determined photometrically after stopping the enzymatic reaction. A working substrate solution was prepared: 0.43 vol of a buffer solution (pH 8.0–8.3) containing 0.5 mol/L glycylglycine was added to a 0.21% solution of γ-L(+)-glutamyl-4-nitroanilide and 0.5 mol/L tris-(hydroxymethyl)-aminomethane (or: dissolve 60 mg of γ-L(+)-glutamyl-4-nitroanilide in 28 ml of distilled water at 80 °C and add 12 ml of a buffer solution (pH 8.0–8.3), containing 0.5 mol/L glycylglycine and 0.5 mol/L *tris*-(hydroxymethyl)-aminomethane). First, 50 μL of the working substrate solution was introduced into microtubes for experimental and blank, calibration, and comparative samples and incubated for 5 min at 37 °C. 50 μL of the medium in which the cells were cultured was added to the experimental samples and incubated for 15 min at 37 °C. 2.5 μL of the prepared calibration solution (*p*-nitroaniline 5.4 mmol/L) was added to the calibration sample, then 300 μL of 10% acetic acid was added to all samples to stop the reaction. 50 μL of culture medium was added to blank samples, 47.5 μL of distilled water was added to the calibration sample, and 50 μL of distilled water to the comparative sample. Incubate for 5 min at room temperature, measure the optical density of the test samples (E_d) against the blank samples, the optical density of the calibration sample (E_{cal}) against the reference sample at 405 nm. The activity of GGT was calculated according to the formula:

$$C = E_d/E_{cal} \cdot 3.0 \ [\mu kat/L]$$

(C is GGT activity, μkat/L; 3 – conversion factor, μkat/L; E_d is the optical density of the test sample, units. wholesale densities; E_{cal} is the optical density of the calibration sample, units. wholesale density).

3. Results and discussion

3.1. Synthesis and structural characterization of Pd(II)/Pt(II) π-complexes

Four novel chelate-type π-coordination compounds were obtained by the reaction of palladium(II) chloride ($PdCl_2$) or potassium tetrachloroplatinate(II) ($K_2[PtCl_4]$) with *N,N*-diethyl-*N'*-(2-propenyl)thiourea (HL^1) or *N*-cyclohexyl-*N'*-(2-propenyl)thiourea (HL^2) in ethanol or water–ethanol solutions according to Scheme 1. A common feature for all synthesized compounds is the same bidentate-chelate coordination of thioureas HL^1 and HL^2 and the structure of the internal coordination sphere of metals: a square-planar coordination unit of palladium or platinum ions is formed by atoms of the S,C-allylthiourea group and chloride anions of the starting metal salt.

At the same time, as shown by X-ray diffraction studies, the coordinated $C^1{-}C^2$ double bond of the allyl moiety is placed perpendicular to the plane of the coordination polyhedron of the central atom (the angles Cl^2-Pd^1-C^1, Cl^2-Pd^1-C^2, Cl^2-Pt^1-C^1 and Cl^2-Pt^1-C^2 are 88.4(3)°, 92.4(2)°, 87.5(2)°, 92.7(1)° respectively, Table S1), which ensures the maximum overlap of the electronic π-orbitals of the ligand with the *d*-orbitals of the metal. The chloride anions are in the *cis*-position of the square-planar polyhedron (Fig. 1a, 2a) similar to the well-known anticancer drug cisplatin. The acidic medium of the synthesis promoted the coordination of thioureas to Pd(II) and Pt(II) ions also in the thione tautomeric form, as evidenced by the C^4–S^1 bond lengths (1.72 and 1.74 Å, Table S1). The thione tautomeric form of thioureas is also evidenced by the valence vibrations ν(C═S) in the IR spectra, which is relevant for complexes **I** and **II**, for which there are no X-ray structural characteristics (Fig. S7).

The asymmetric unit of compounds **III** and **IV** contains one molecule of the complex with a solvate water molecule (Fig. 1a, 2a). The central metal ion forms a slightly deformed square-planar coordination polyhedron $M(C^1{-}C^2)SCl_2$ due to coordination by thiourea sulfur S^1, two chloride ions Cl^1, Cl^2 and the double bond C^1–C^2 of the allylic moiety.

The metal atom and the sulfur, and two chlorine atoms lie within the plane with accuracy of 0.032 Å in complex **III** and 0.035 Å in complex **IV**. The angle between the plane of the coordination polyhedron and the C^1–C^2 double bond is 80.5° in complex **III** or 83.3° in the complex **IV**.

The formation of coordinate bond with the sulfur atom leads to the elongation of the C^4–S bond (compared to the non-coordinated thioureas [42]), (Table S1). At the same time, the $M{-}Cl^2$ bond (which is on diagonal to the C^4–S double bond) in both complexes is slightly longer than $M{-}Cl^1$ by 0.039 (complex **III**) and 0.018 Å (complex **IV**) which can be explained by the probable repulsion of two identical anions that are placed in the same plane, as well as by the influence of a strong *trans*-effect in the allylic moiety.

The C^1–C^2 double bond of the coordinated allylic moiety is close to the mean value of terminal $C_{sp2}{=}C_{sp2}$ bond [62] of 1.299 Å in complex **III** (1.311(14) Å) and is elongated in complex **IV** (1.405(7) Å). The Pt–C bond lengths are slightly shorter than compared to Pd–C ones (Table S1) that can be explained by the slightly larger ionic radius of Pd^{2+} (0.64 Å) compared to Pt^{2+} (0.6 Å). The $M{-}C^2{-}C^3{-}N^1{-}C^4$–S metallocycle adopts a twist-boat conformation in both complexes. The cyclohexane ring of HL^2 adopts a chair conformation in two complexes under study.

In the crystal phase, complexes **III** and **IV** are bound through the bridged water molecules due to the N^1–H…$O^{1w'}$ and O^{1w}–H…$Cl^{2'}$ hydrogen bonds (Table S2) forming the centrosymmetric tetramers (Fig. 1b, 2b).

These tetramers are bound by weaker O^{1w}–H…$Cl^{1'}$, O^{1w}–H…S1′ and N^2–H…$Cl^{2'}$ hydrogen bonds (Table S2) that results in the formation of layers parallel to the (0 0 1) crystallographic plane (Fig. 3 *a, b*).

Complexes **I**, **II** have a similar structure to complexes **III**, **IV**, as

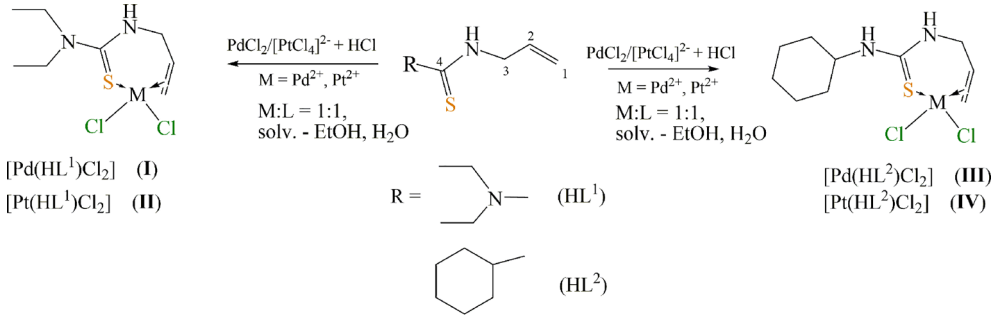

Scheme 1. Synthesis of Pd(II) and Pt(II) complex compounds **I–IV.**

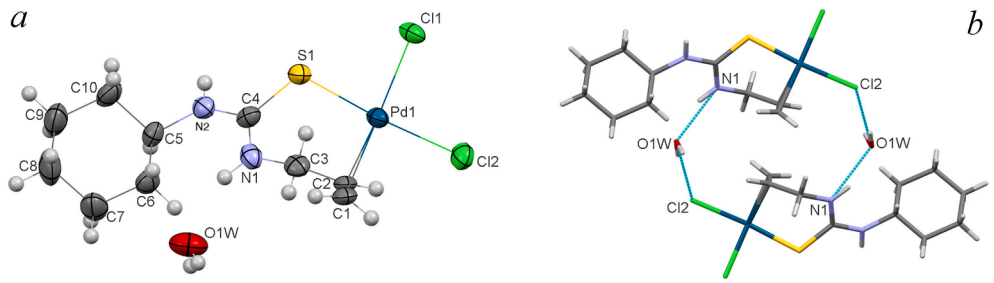

Fig. 1. Molecular structure of complex **III** with the thermal displacements of non-hydrogen atoms at the 50% probability level (*a*) and the dimer of complex molecules formed through the bridged water molecules (*b*).

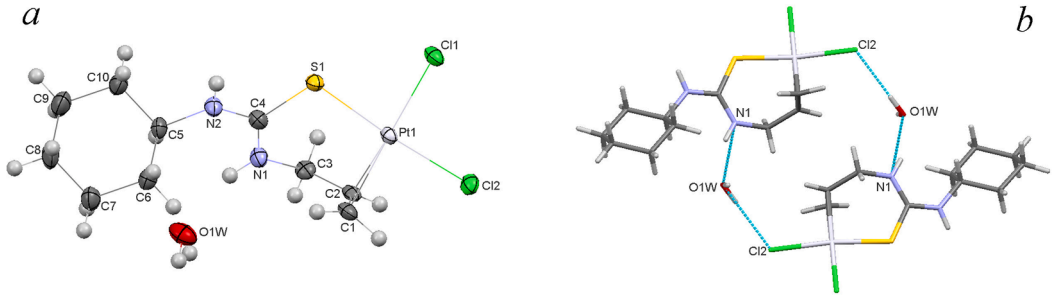

Fig. 2. Molecular structure of complex **IV** with the thermal displacements of non-hydrogen atoms at the 50% probability level (*a*) and the dimer of complex molecules formed through the bridged water molecules (*b*).

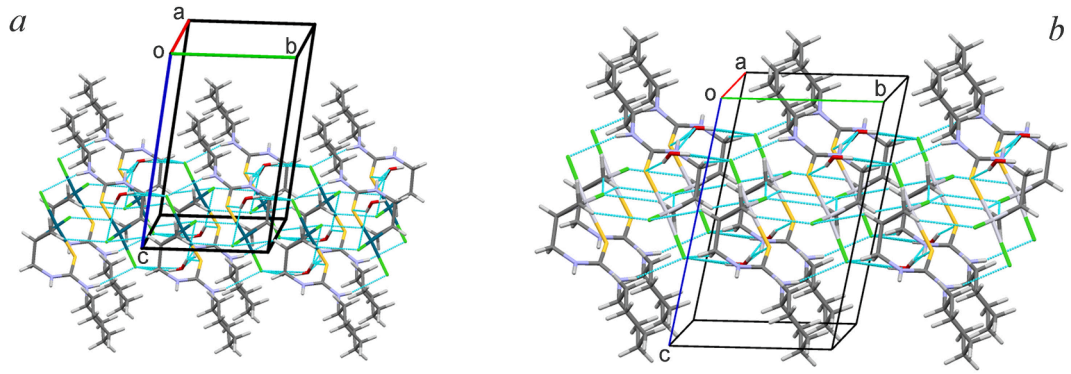

Fig. 3. Layers of complexes **III** (*a*) and **IV** (*b*). Hydrogen bonds are shown by dashed cyan lines.

evidenced by the $^{1}H/^{13}C$ NMR, IR, and UV–vis spectral data presented below.

All synthesized π-coordination compounds decompose at t > 215–300 °C. They are soluble in acetone, acetonitrile, pyridine, DMSO, DMF, and slightly soluble in water and ethanol (only when heated with a concentration of 10^{-3} mol/L).

3.2. $^{1}H/^{13}C$ NMR spectroscopic characterization of HL^{1}, HL^{2} and complexes I–IV

A comparison of the ^{1}H NMR spectra of the synthesized n,π-chelate complexes with the spectra of thioureas $HL^{1,2}$ showed that the most sensitive to complex formation are the proton signals of NH groups that are in proximity to C═S, which is involved in the formation of a bond with a metal ion, and also protons of the allylic moiety, which participate in the formation of the π-coordination bond and are part of the metallocycle (Fig. S1, S2; Tables S3, S4).

Similar to previous studies [42,44], the signals of NH protons undergo a significant downfield shift by $\Delta\delta_H$=+(1.279–1.934) ppm, while the protons of the allylic moiety $=C^{1}H_{trans}$ and $=C^{1}H_{cis}$ shift into the upfield by $\Delta\delta_H$= -(0.123–1.503) ppm (Tables S3, S4). This is due to the proximity of the $N^{1}H$ and $N^{2}H$ groups to the donor–acceptor bond (C═S)→Pd/Pt and the formation of the π-coordination bond (C^{1}=C^{2})→Pd/Pt.

In addition, the protons of the $=C^{2}H$ group undergo a significant shift, which is associated with a large contribution of the π-acceptor component to the formation of the π-coordination bond. The unoccupied π*-loosening electronic orbital of the C═C double bond overlaps with the filled *d*-orbital of the Pd^{2+} or Pt^{2+} ion, which leads to an increase in the electron density on the atoms of the allyl fragment, and therefore to their shielding. At the same time, the multiplet signal of the proton $=C^{2}H$ in Pd(II) complexes shifts to the downfield ($\Delta\delta_H$=+(0.308–0.305), and in Pt(II) complexes – to the up one ($\Delta\delta_H$ = -0.817 ppm (Tables S3, S4) which is indicative of the influence of the nature of metal on the spectral characteristics of complexes.

The entry of the $C^{3}H_2$ group of the allylic moiety into the metallocycle leads to the splitting of a broad multiplet (4.172 and 4.042 ppm in the ^{1}H NMR spectra of thioureas HL^{1} and HL^{2}) into two doublets with corresponding spin–spin interaction constants of almost the same value (Fig. 4, S1, S2 and Tables S3, S4). This is due to the axial and equatorial

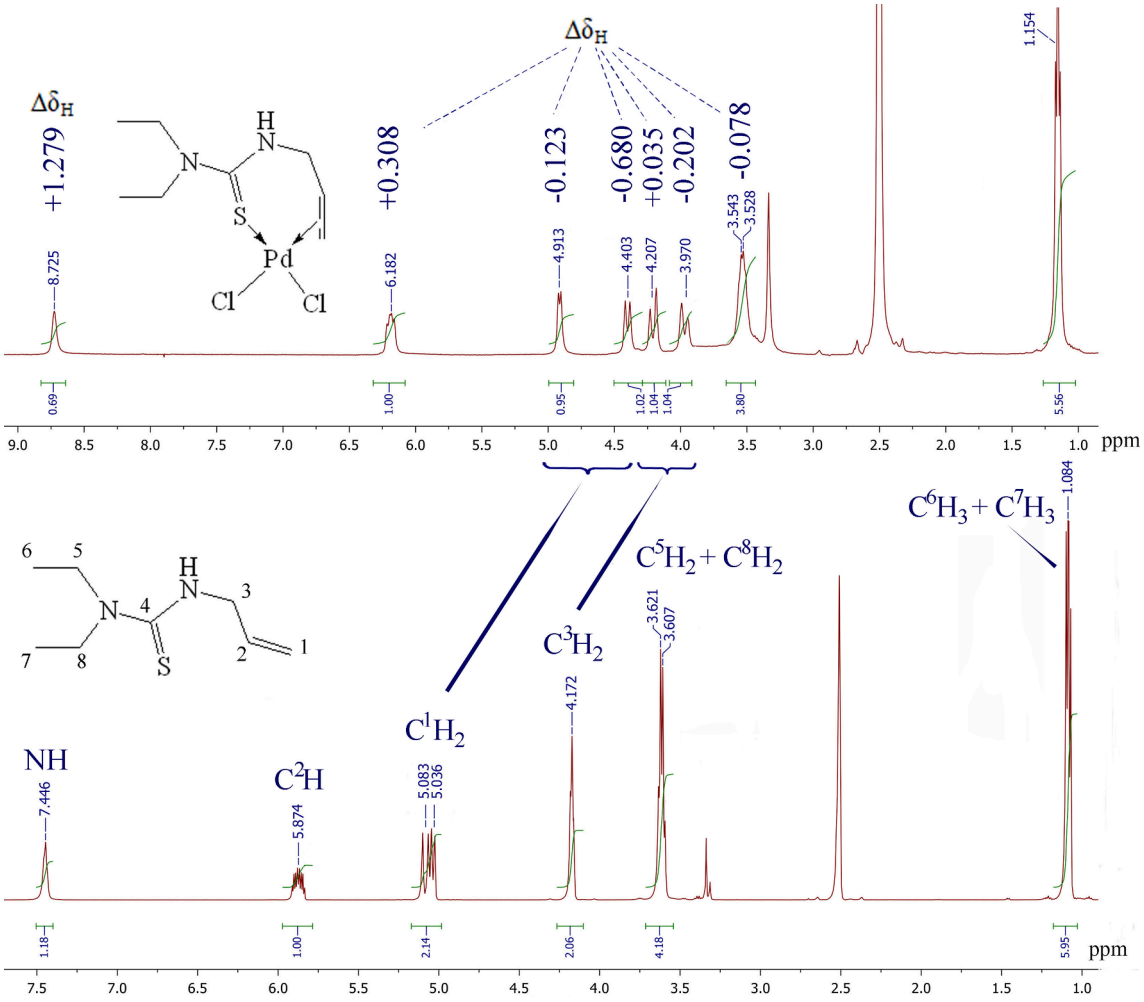

Fig. 4. ^{1}H NMR spectra of starting *N*,*N*-diethyl-*N'*-(2-propenyl)thiourea HL^{1} and complex **I**.

position of these protons in the metallocycle of the complexes [51,42,44]. It should be noted that the splitting of protons of the C^3H_2 group is a characteristic indicator of the formation of a chelate metallocycle, which makes the ^{1}H NMR method very convenient for studying the structure of such compounds.

The study of the NMR spectra of the synthesized π-complexes in DMSO is relevant as it is known [63] that DMSO inactivates cisplatin and carboplatin because Pd(II) and Pt(II) ions have a high affinity for donor sulfur atoms. As in the previous works [42,44], the obtained results showed that they are stable in this solvent. At the same time, it should be noted that the synthesized complexes are stable for a long time (up to 2 months), as evidenced by the absence of significant signs of decomposition (Fig. S3, *a, b* and S4 *a, b*). Also, this confirms our idea about the stability of synthesized compounds in thiol-containing blood environments. However, the spectrum obtained from the same NMR tube three months later clearly shows that the Pd(II) complex decomposes very slowly in DMSO. The signals of the complex are still present after three months, but a lot of unidentified "garbage" appears (Fig. S3, *c*). This is not surprising, taking into account the high reactivity of palladium complexes. It should be noted that platinum π-complexes are more stable in DMSO. As shown in Fig. S3a and S4a, in two months the NMR spectra are almost the same. According to this, it is possible to use DMSO both to dissolve samples and even to store complexes in it for some time, although more detailed study is required.

In the ^{13}C NMR spectra of the complexes, the signals of carbons C^1, C^2, and C^4 undergo the most significant shift in relation to the starting thioureas (Table S5, Fig. S5, S6). At the same time, the participation of C^4=S in coordination to the central metal ion determines the upfield chemical shift of C^4 only by $\Delta\delta_C$=-(9.68–16.15) ppm. Instead, the participation of C^1=C^2 in the formation of a π-acceptor bond with a metal ion causes a significant chemical shift of the signals of these carbons ($(\Delta\delta_C$=-(32.56–56.32) ppm) in the upfield, which is also indicative for establishing the structure similar compounds [42,44]. At the same time, in the ^{13}C NMR spectrum of platinum complexes, they undergo a much larger shift compared to the spectra of palladium complexes, which is probably due to a higher acceptor capacity of platinum ions.

3.3. IR, UV–vis spectra of thioureas HL^1, HL^2 and complexes I–IV

Despite the possibility of thione-thiol tautomerism for the thioureas used, in the solid state they are in the thione form, as evidenced by the absence of ν(S—H) valence vibrations in the region of 2600–2540 cm^{-1} in the IR spectra (Fig. S7) [51–54].

Unlike complexes with a chelate mode of ligand coordination, the formation of a metallocycle with coordination bonds Pd←S, Pd←C_{allyl}, Pt←S, Pt←C_{allyl} is peculiarly affected on the IR spectra of the synthesized π-complexes (Fig. S7). Usually, the formation of a chelate metallocycle is accompanied by a shift of the characteristic absorption bands to the low-frequency region [52,34,37]. However, in the synthesized n,π-complexes, a slightly different trend in the changes that occurred is observed.

Similar to previous studies [44,48], the absorption bands of valence vibrations ν(NH) and $\nu_{as/s}(CH)_{allyl}$ of the allyl fragment are shifted to the high-frequency region in the IR spectra of complexes **I–IV** (by Δν=+20/

+30/+39/+66 and + 30/+40/+55/+62 cm^{-1} respectively). It is caused by the participation of the allylthioureide group in the formation of a coordination bond with the metal ions. Bands of δ(NH) deformation vibrations also undergo a similar high-frequency shift (Δδ=+27/+30/+28/+18 cm^{-1}), that is characteristic only for π-complexes and distinguishes these IR-characteristics from the spectra of complexes with chelate coordination of ligands. However, the valence vibrations of ν(C═S) undergo a low-frequency shift by $\Delta\nu$ = -47/-42/-44/-40 cm^{-1} (Fig. S7), that is inherent in the chelate coordination of the carbothioamide group.

The UV–vis spectra of thioureas HL^1, HL^2 free from coordination (dissolved in a DMF-ethanol mixture) are not very informative (Fig. 5 *a, b*) due to the influence of the solvent. Basically, they consist of shoulder-shaped weakly pronounced absorption bands (ABs) due to intraligand n→π* electronic transitions, which relate to the contributions of the C═S multiple bond of the thiourea group [51]. At the same time, the positions of their maxima differ by $\Delta\lambda = 6$ nm, which is due to the effect of the nature of the substituent in the HL^1 and HL^2 molecules, despite their aliphatic nature in both thioureas. However, the spectra of ethanol solutions of thioureas are slightly differed (Fig. S8).

In the spectra of the complexes, there are absorption bands that are responsible for electronic transitions with ligand to the metal charge transfer (LMCT) and *dd*-electronic transitions (Fig. 5 *a,b*). In platinum complexes **II** and **IV**, a broad absorption band at 307/305 nm corresponds to the overlapping of n→π* intraligand electronic transitions with LMCT. And in palladium complexes **I**, **III**, the LMCT absorption bands (370/365 nm) and *dd*-electronic transitions (465/470 cm^{-1}) are visualized, that is due to the effect of the nature of the metal.

To analyze of complex formation in ethanol solution, the dependence of the optical density on the ligand concentration was studied (Fig. S8). In contrast to the spectra of the synthesized complexes dissolved in a mixture of DMF:ethanol = 2:1 (Fig. 5), in the UV–vis of water–ethanol solutions of the complexes (obtained *in citu*, Fig. S8) the absorption bands of intraligand π→π*, n→π* electronic transitions (248, 265/246, 259, 275/267, 287/243, 255 nm), LMCT (320/312, 348/317, 368/282, 310 nm) and *dd* (398/385/398/386 nm) are observed in hypsochromic shift relative to the previous spectra that caused by the different nature of the solvent. The results showed that the titration curves have slightly pronounced inflections at the ratio M:L = 1:1, 1:2 and 1:3, which indicates the possible coordination of ligands in the solution in both a chelate and non-chelate manner only through the sulfur atoms of the carbothioamide group. Despite this, only complexes with the 1:1 ratio were isolated in the solid state, which is caused by the Pearson's effect, that is, the strong *trans*-influence of the allylic moiety, which destabilizes the bond with a "soft" atom in the *trans*-position.

3.4. Biological study

The use of n,π–chelate complexes of Pd(II) and Pt(II) can help in solving the problem of cell resistance to anticancer drugs - analogues of cisplatin, caused by the binding of their active complexes to thiol-containing substances in the cytoplasm of blood [64], which is one of the mechanisms of resistance of pathogenic cells to the action of platinum drugs.

3.4.1. *Effect of Pt(II) and Pd(II) π-complexes on the growth of multicellular spheroids of MCF-7 breast tumor cells*

Multicellular tumor spheroids are aggregates of tumor cells that are formed *in vitro* due to the conversion of adherent cells and better reproduce the growth characteristics of solid tumors in vivo, which are locally characterized by hypoxia, acidosis and lack of nutrients, which leads to genetic and adaptive changes in the tumor [65]. Spheroids grown from cancer cell lines have tumor-like characteristics, which may reflect their clinical significance [66,67], and then apply them to drug screening and to develop individualized diagnostic and treatment methods. In recent years, a spheroid model produced by three-dimensional (3D)-culture has attracted attention as a better experimental model that is closer to the physiological environment in vivo.

MCF-7 breast adenocarcinoma is the most appropriate model for studying the effect of novel substances on their aggregation, adhesion, etc. Spheroid growth characterizes the metastatic potential of cells.

The size distribution of spheroids under the influence of complexes was determined in five ranges: 20–170 μm^2, 170–500 μm^2, 500–850 μm^2, 850–1350 μm^2, 1350–1700 μm^2 and more. Under the action of complex **I**, an increase in the percentage of spheroids with an area of 170–500 μm^2 is observed, and the share of spheroids with the smallest dimensions (20–170 μm^2) gradually decreases with the time of incubation. This indicates that individual cells are not separated from the spheroids and have a reduced ability to metastasize as a result of the action of this complex (Fig. 6).

When complex **II** was added, there was also a slight increase in the percentage of spheroids with an area of 500–850 μm^2 on the sixth and seventh days of cultivation and a decrease in the percentage of spheroids with an area of 20–170 μm^2. However, there was no reliable stimulation of spheroid growth. Under the influence of complex **III**, a decrease in the number of spheroids with an area of 20 – 170 μm^2 was observed. Therefore, it can be assumed that this compound shows a slight stimulation of the growth of spheroids. The growth of spheroids wasn't observed under the influence of compound **IV**, as well as under the influence of *cis*platin. However, there was a slight decrease in the number of spheroids with an area of 20–170 μm^2. At the same time, the area of spheroids remained relatively constant even in the control. Therefore, it can be concluded that under the influence of the studied complexes **I**–**IV** and cisplatin, the number of the smallest spheroids (with an area of

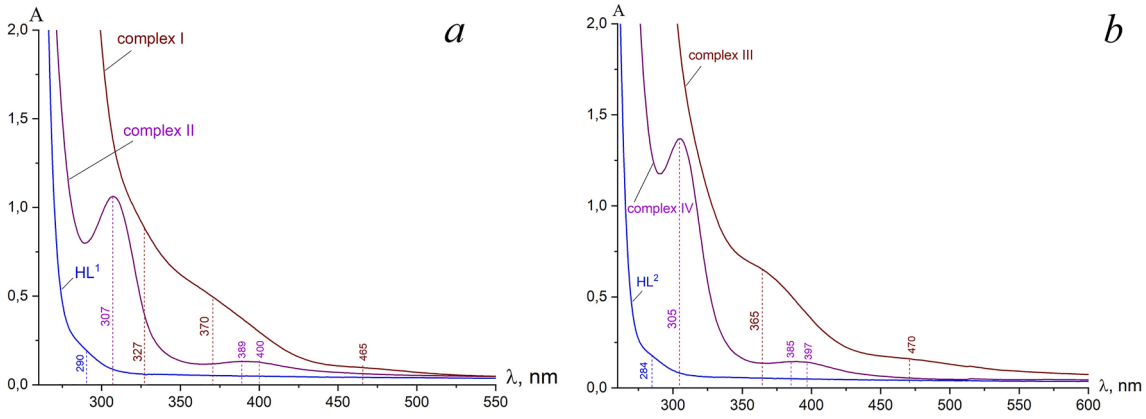

Fig. 5. The UV–vis spectra of thioureas $HL^{1,2}$ and complexes **I**, **II** (*a*) and **III**, **IV** (*b*) in DMF-ethanol (2:1) mixture solution.

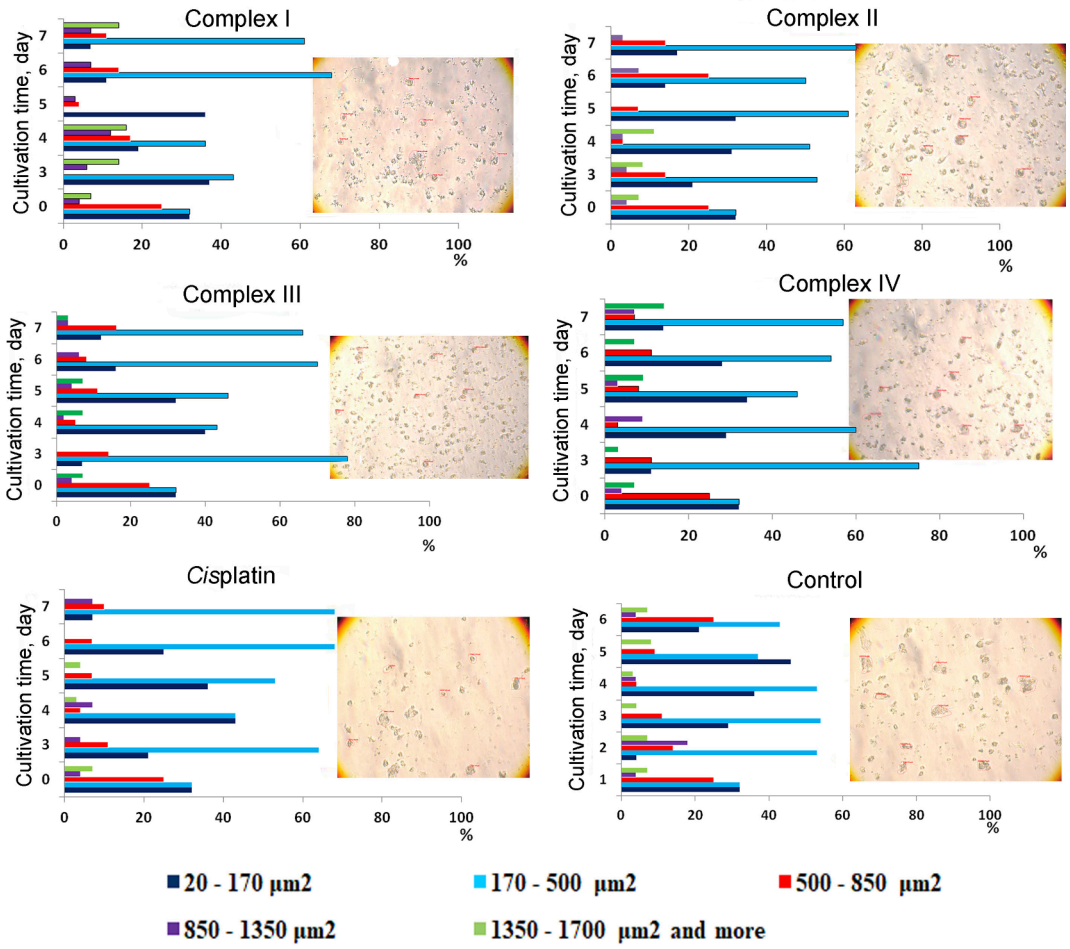

Fig. 6. MCF-7 spheroid area distribution under the effect of complexes **I**–**IV** and *cis*platin (*hereinafter: M ± m, n = 5*).

20–170 μm^2) decreased, the population of attached cells grew, and the total content of living cells decreased compared to the control (without the addition of synthesized compounds).

After determining the size of the spheroids on the 7th day of cultivation, the adhesion index of cells to the substrate was determined. The index of cell adhesion in the control was taken as 100% (Fig. 7). As shown by the given data, the adhesion index on the 7th day of cultivation of the spheroid culture under the influence of complex **I** increased by 1.25 times compared to the control and by 1.5 times compared to cisplatin. The adhesion index under the influence of all studied complexes was higher by 17–50% compared to *cis*platin (Fig. 7).

Also, under the influence of complexes **IV** and **II**, it was possible to observe the morphofunctional similarity of the attached cells to the control, namely the elongation of cells with an epithelial-like structure and polar processes. This indicated the inversion of the small cell structure of tumor cells in the direction of differentiation. Under the action of complex **I**, for which the highest adhesion index was recorded, most of the cells had a rounded shape, but were fixed on the substrate.

In a comparative study of the effects of cisplatin in 2D and 3D culture, greater efficacy was recorded for 3D culture, as the antitumor efficacy of cisplatin is associated with the activation of pro-apoptotic action mediated by caspase 3 and E-cadherin. A decrease in the size of spheroids due to an increase in the level of apoptosis was recorded under the influence of cisplatin [68]. In our studies, under the action of synthesized complexes **I** and **III**, a decrease in the size of spheroids during long-term cultivation was also observed, especially on the 7th day of cultivation, which may also indicate an intensification of the proapoptotic effect. Also, 3D culture makes it possible to record the influence of the microenvironment on the size and proliferative indicators of the spheroid micronode.

3.4.2. Gamma-glutamyl transpeptidase (GGT) enzyme activity on MCF-7 microspheroids cells under the action of n,π-chelate complexes I–IV

It is known that the main target of action of cisplatin and its structural analogues, in addition to a number of receptor molecules, is human gamma-glutamyltranspeptidase-1 (GGT1). This enzyme plays a leading role in the metabolism of the antioxidant glutathione, which provides detoxification, protection against reactive oxygen species and prevents oxidative stress in cells. When using certain chemotherapy drugs, this enzyme is induced, as a result of which inactive complexes with glutathione and its derivatives are formed and drug resistance occurs. Therefore, in this subsection, the research was focused on determining the effect of synthesized complexes **I**–**IV** on GGT activity of MCF-7 microspheroids.

On the 7th day in the cultivation medium, GGT activity was determined in the control and under the influence of the complexes **I**–**IV** (Fig. 8). The results showed that, unlike cisplatin (under the influence of which the activity of GGT increased 1.3 times compared to the control), all π-complexes did not increase the activity of GGT, but inhibited the activity of this enzyme.

Under the influence of complexes **I** and **III**, the activity of GGT decreased by 1.25 and 1.4 times, respectively, compared to the control. At the same time, GGT activity under the influence of substances **II** and **IV** is almost 2 times lower than under the influence of cisplatin. Therefore, it can be assumed that the investigated n,π-complexes do not cause drug resistance of transformed cells, mediated by GGT activity.

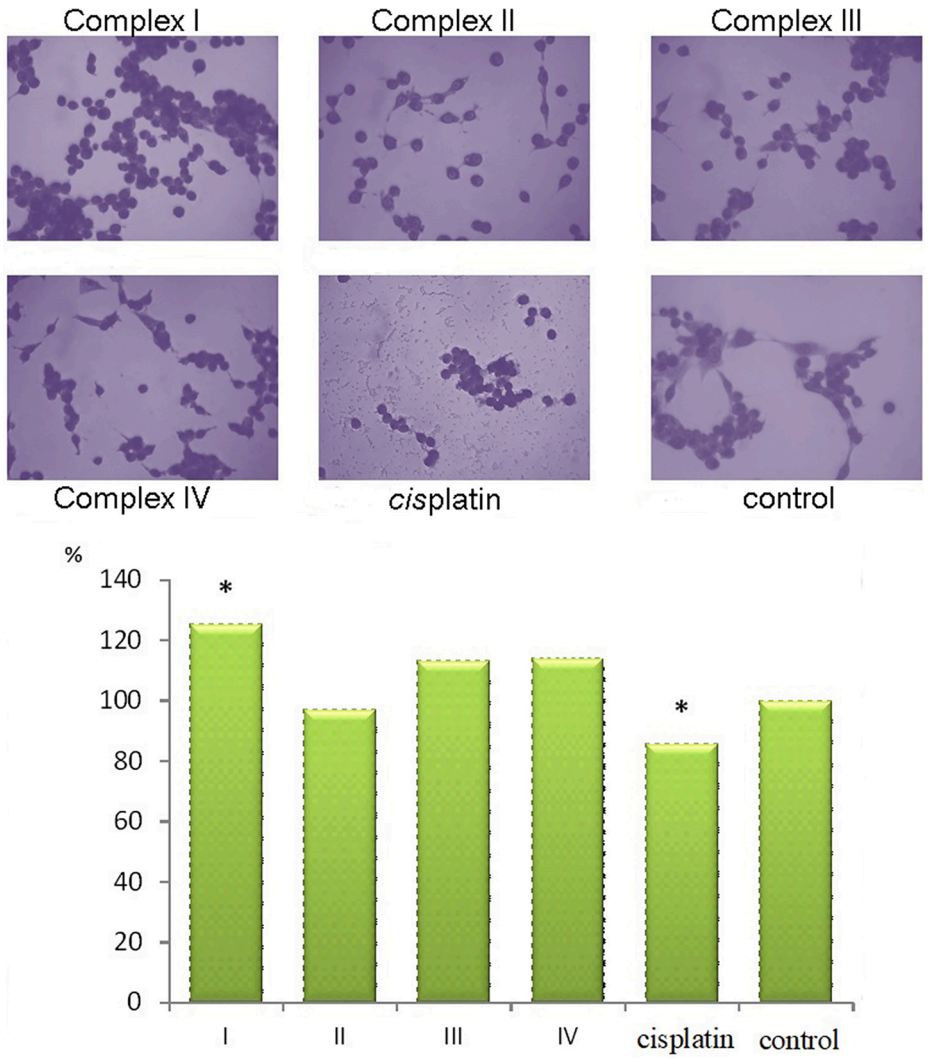

Fig. 7. Adhesive properties of MCF-7 cells spheroids after 7 days cultivation with complexes **I**–**IV** and *cis*platin (adhesive index in the control equals 100%).

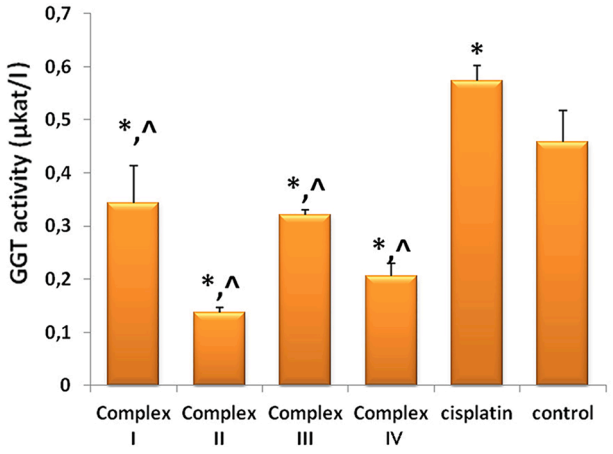

Fig. 8. GGT activity under the influence of complexes **I**–**IV** and cisplatin on the 7th day cultivation MCF-7 (*– $p < 0.05$, *vs* control;^ – *vs* cisplatin).

Thus, we have shown a decrease in the level of GGT activity, as the main enzyme involved in the formation of drug resistance, when using the classic chemo drug cisplatin. As evidenced by the above data, both compared to cisplatin and the control, all four novel synthesized complexes inhibit the activity of GGT, which is one of the important mechanisms for preventing drug resistance.

4. Conclusion

Four novel n,π-chelate complexes of Pd(II) and Pt(II) with general formula $[M(HL^{1,2})Cl_2]$ ($HL^{1,2}$ – *N,N*-diethyl-*N'*-(2-propenyl)thiourea and *N*-cyclohexyl-*N'*-(2-propenyl)thiourea) were synthesized. All compounds were investigated by nuclear magnetic resonance ($^1H/^{13}C$ NMR), UV–vis and infrared spectroscopy. Two structures were characterized by X-ray diffraction method.

It was established that palladium and platinum π-complexes have a similar molecular and crystalline structure. The metal ions are coordinated by the thiourea sulfur atom and the terminal double (C═C) bond of the allylic moiety with the formation of a six-membered chelate metallocycle which is in a twist-boat conformation. The Pd^{2+} and Pt^{2+} cations have a square-planar environment. In the crystal, both complexes exist in the form of monohydrate.

It was found that the obtained compounds are stable in DMSO, and it was shown that $^1H/^{13}C$ NMR spectroscopy is a convenient method for studying the structure of π-coordination compounds. It was established that the splitting of the CH_2 proton signals of the allylic moiety in the ^1H NMR spectra into two doublets characterizes the formation of a chelate metallocycle.

It was shown that in the IR spectra of the synthesized complexes, the

absorption bands of ν(NH), $\nu_{as/s}(CH)_{allyl}$ and δ(NH) undergo a significant high-frequency shift, which is a distinctive feature from the IR spectra of other coordination compounds with chelate coordination of ligands.

It was established that, despite the isolation of complexes only in the ratio M:L = 1:1, compounds with a stoichiometric ratio M:L = 1:1, 1:2, 1:3 can be formed in the solution, as evidenced by titrimetric curves of complexometric study in water–ethanol solutions. The formation of such compounds in solution is possible under conditions of monodentate coordination of HL^1 and HL^2.

Studies of the effects of the complexes on MCF-7 cells culture spheroids showed that they exhibit a pronounced antimetastatic activity, which causes a decrease in the number of the smallest spheroids (with an area of 20–170 μm^2), an increase in the population of attached cells and a general decrease in the content of living cells compared to the control. The hypothesis that the greater proapoptotic activity of n,π-chelate complexes Pd(II) and Pt(II) compared to cisplatin is caused by their inhibitory properties was confirmed.

It was found that complexes based on diethyl-substituted carbothioamide are more active compared to complexes based on cyclohexyl-substituted carbothioamide, but in general, the studied compounds are more active compared to classic chemo drug cisplatin both in terms of the effect on the adhesive properties of MCF-7 cell spheroids and the level of GGT activity.

Declaration of Competing Interest

The authors declare that they have no known competing financial interests or personal relationships that could have appeared to influence the work reported in this paper.

Data availability

Data will be made available on request.

Acknowledgment

The publication contains the results of studies performed with the financial support of NAS of Ukraine (according to fundamental research on the topic 321 E of the V.I. Vernadsky Institute of General and Inorganic Chemistry NAS of Ukraine). The X-ray diffraction study is supported by the NAS of Ukraine (project 0122U200071).

Appendix A. Supplementary data

Supplementary data to this article can be found online at https://doi.org/10.1016/j.poly.2022.116272.

References

[1] I.L. Goncalves, G.O. de Azambuja, D.F. Kawano, V.L. Eifler-Lima, Thioureas as building blocks for the generation of heterocycles and compounds with pharmacological activity: An overview, Mini-Rev. Organ. Chem. 15 (2018) 28–35, https://doi.org/10.2174/1570193X14666170518125219.

[2] H. Eshghi, M. Bakavoli, J. Abedini-Torghabeh, M. Rahimizadeh, A. Keykha, Synthesis of heterocyclic compounds by reaction of dialkyl acetylenedicarboxylates with thiourea derivatives, Heterocycl. Commun. 19 (2013) 271–274, https://doi.org/10.1515/hc-2013-0041.

[3] H.I. Severina, O.O. Skupa, N.I. Voloshchuk, A.R. Khairulin, V.A. Georgiyants, Design, synthesis, in vivo and in silico anticonvulsant activity studies of derivatives of 6-amino-4-hydroxy-2-thio-pyrimidine, Acta Pharm. Sci. 58 (2020) 371–393. http://dspace.nuph.edu.ua/handle/123456789/26718.

[4] Y.L. Zborovskii, V.V. Orysyk, V.I. Staninets, V.V. Bon, Halocyclization of 2-(2-{4-[allylamino(thioxo)methyl]piperazin-1-yl}ethyl)-1*H*-benzo[*de*]isoquinoline-1,3(2*H*)-dione, Russ. J. Org. Chem. 47 (2011) 881–885, https://doi.org/10.1134/S107042801106008X.

[5] V.B. Bregović, N. Basarić, K. Mlinarić-Majerski, Anion binding with urea and thiourea derivatives, Coord. Chem. Rev. 295 (2015) 80–124, https://doi.org/10.1016/j.ccr.2015.03.011.

[6] V. Kumar, S.S. Chimni, Recent developments on thiourea based anticancer chemotherapeutics, Anti-Cancer Agents Med. Chem. 15 (2015) 163–175, https://doi.org/10.2174/1871520614666140407123526.

[7] S.K. Pandey, S. Pratap, G. Gozzi, G. Marverti, R.J. Butcher, Synthesis, molecular structure exploration and in vitro cytotoxicity screening of five novel *N*, *N'*-disubstituted thiocarbamide derivatives, Phosphorus Sulfur Silicon Relat. Elem. 193 (2018) 507–514, https://doi.org/10.1080/10426507.2018.1452234.

[8] O.J. D'cruz, F.M. Uckun, Novel tight binding PETT, HEPT and DABO-based non-nucleoside inhibitors of HIV-1 reverse transcriptase, J. Enzyme Inhib. Med. Chem. 21 (2006) 329–350, https://doi.org/10.1080/14756360600774413.

[9] C. Sun, X. Zhang, H. Huang, P. Zhou, Synthesis and evaluation of a new series of substituted acyl(thio)urea and thiadiazolo [2,3-*a*] pyrimidine derivatives as potent inhibitors of influenza virus neuraminidase, Bioorg. Med. Chem. 14 (2006) 8574–8581, https://doi.org/10.1016/j.bmc.2006.08.034.

[10] J. Stefańska, K. Stępień, A. Bielenica, M. Wrzosek, M. Struga, Antistaphylococcal activity of selected thiourea derivatives, Polish, J. Microbiol. 65 (2016) 451–460, https://doi.org/10.5604/17331331.1227671.

[11] A. Liav, S.K. Angala, P.J. Brennan, M. Jackson, *N*-D-Aldopentofuranosyl-*N'*-[p-(isoamyloxy)phenyl]-thiourea derivatives: Potential anti-TB therapeutic agents, Bioorg. Med. Chem. Lett. 18 (2008) 2649–2651, https://doi.org/10.1016/j.bmcl.2008.03.033.

[12] S.A. Khan, N. Singh, K. Saleem, Synthesis, characterization and *in vitro* antibacterial activity of thiourea and urea derivatives of steroids, Eur. J. Med. Chem. 43 (10) (2008) 2272–2277, https://doi.org/10.1016/j.ejmech.2007.12.012.

[13] M. Huang, M. Huang, X. Wang, W.-G. Duan, G.-S. Lin, F.-H. Lei, Synthesis, antifungal activity and 3D-QSAR study of novel acyl thiourea compounds containing *gem*-dimethylcyclopropane ring, Mol. Div. 26 (2022) 125–136, https://doi.org/10.1007/s11030-020-10163-6.

[14] H. Wang, Z.-W. Zhai, Y.-X. Shi, C.-X. Tan, J.-Q. Weng, L. Han, B.-J. Li, X.-H. Liu, Novel trifluoromethylpyrazole acyl thiourea derivatives: Synthesis, antifungal activity and docking study, Lett. Drug Des. Discov. 16 (2019) 785–791, https://doi.org/10.2174/1570180815666180704103047.

[15] W. Bai, J. Ji, Q. Huang, W. Wei, Synthesis and evaluation of new thiourea derivatives as antitumor and antiangiogenic agents, Tetrahedron Lett. 61 (2020), 152366, https://doi.org/10.1016/j.tetlet.2020.152366.

[16] M. Tapera, H. Kekeçmuhammed, K. Sahin, V.S. Krishna, C. Lherbet, H. Homberset, M. Chebaiki, T. Tønjum, L. Mourey, Y.u. Zorlu, S. Durdagi, E. Sarıpınar, Synthesis, characterization, anti-tuberculosis activity and molecular modeling studies of thiourea derivatives bearing aminoguanidine moiety, J. Mol. Struct. 1270 (2022), 133899, https://doi.org/10.1016/j.molstruc.2022.133899.

[17] T. Yeşilkaynak, F.N. Özkömeç, M. Çeşme, R.E. Demirdöğen, E. Kutlu, H.M. Kutlu, F. M. Emen, Synthesis of new thiourea derivatives and metal complexes: Thermal behavior, biological evaluation, *in silico* ADMET profiling and molecular docking studies, J. Mol. Struct. 1269 (2022), 133758, https://doi.org/10.1016/j.molstruc.2022.133758.

[18] A. Shahzad, E. Khan, M. Said, G.S. Khan, M.G. Syed, A. Noor, M. Zahoor, R. Ullah, A. Bari, Complexes of 1,3-diisobutyl thiourea with copper(I), zinc(II) and mercury (II): Their antioxidant and antibacterial evaluation, Crystals 11 (2021) 989, https://doi.org/10.3390/cryst11080989.

[19] I.I. Ozturk, S. Yarar, C.N. Banti, N. Kourkoumelis, M.P. Chrysouli, M. Manoli, A. J. Tasiopoulos, S.K. Hadjikakou, QSAR studies on antimony(III) halide complexes with N-substituted thiourea derivatives, Polyhedron 123 (2017) 152–161, https://doi.org/10.1016/j.poly.2016.11.008.

[20] M. Monim-ul-Mehboob, M. Akkurt, I.U. Khan, S. Sharif, I. Asif, S. Ahmad, Hexakis (thiourea-*κ*S)nickel(II) nitrate: a redetermination, Acta Cryst. E 66 (2010) i57–i58, https://doi.org/10.1107/S1600536810026668.

[21] S. Nadeem, M.K. Rauf, M. Bolte, S. Ahmad, S.A. Tirmizi, M. Asma, A. Hameed, Synthesis, characterization and antibacterial activity of palladium(II) bromide complexes of thioamides; X-ray structure of $[Pd(tetramethylthiourea)_4]Br$ 2, Trans. Met. Chem. 35 (2010) 555–561, https://doi.org/10.1007/s11243-010-9363-0.

[22] M.C. Risi, G.C. Saunders, W. Henderson, The coordination chemistry of sulfonyl-substituted thioureas towards the d^8 metal centres platinum(II), palladium(II), nickel(II) and gold(III), Inorg. Chim. Acta 526 (2021), 120506, https://doi.org/10.1016/j.ica.2021.120506.

[23] A.M. Plutín, R. Ramos, R. Mocelo, A. Alvarez, E.E. Castellano, M.R. Cominetti, K. M. Oliveira, T.D. de Oliveira, T.E.M. Silva, R.S. Correa, A.A. Batista, Antitumor activity of Pd(II) complexes with N, S or O, S coordination modes of acylthiourea ligands, Polyhedron 184 (2020), 114543, https://doi.org/10.1016/j.poly.2020.114543.

[24] B.N. Cunha, L. Colina-Vegas, A.M. Plutin, R.G. Silveira, J. Honorato, K.M. de Oliveira, M.R. Cominetti, A.G. Ferreira, E.E. Castellano, A.A. Batista, Hydrolysis reaction promotes changes in coordination mode of Ru(II)/acylthiourea organometallic complexes with cytotoxicity against human lung tumor cell lines, J. Inorg. Biochem. 186 (2018) 147–156, https://doi.org/10.1016/j.jinorgbio.2018.06.007.

[25] A. Singh, M.K. Bharty, P. Bharati, A. Bharti, S. Singh, N.K. Singh, Synthesis, spectral, thermal and structural characterization of a hexanuclear copper(I) cluster and a cobalt(III) complex of 1-ethyl-3-phenyl-thiourea, Polyhedron 85 (2015) 918–925, https://doi.org/10.1016/j.poly.2014.10.018.

[26] A. Noor, S. Qayyum, F. Jabeen, A.U. Rehman, Mononuclear tricoordinate copper(I) and silver(I) halide complexes of a sterically bulky thiourea ligand and a computational insight of their interaction with human insulin, Molecules 27 (2022) 4231, https://doi.org/10.3390/molecules27134231.

[27] W. Henderson, B.K. Nicholson, M.B. Dinger, R.L. Bennett, Thiourea monoanion and dianion complexes of rhodium(III) and ruthenium(II), Inorg. Chim. Acta 338 (2002) 210–218, https://doi.org/10.1016/S0020-1693(02)01017-4.

[28] T.S. Smith, W. Henderson, B. Rian, K. Nicholson, Cycloaurated gold(III) complexes with monoanionic thiourea ligands, Inorg. Chim. Acta 408 (2013) 27–32, https://doi.org/10.1016/j.ica.2013.07.027.

[29] A. Saeed, M.N. Mustafa, M. Zain-ul-Abideen, G. Shabir, M.F. Erben, U. Flörke, Current developments in chemistry, coordination, structure and biological aspects of 1-(acyl/aroyl)-3-(substituted)thioureas: advances Continue, J. Sulfur Chem. 40 (2019) 312–350, https://doi.org/10.1080/17415993.2018.1551488.

[30] A. Lapasam, M.R. Kollipara, A survey of crystal structures and biological activities of platinum group metal complexes containing *N*-acylthiourea ligands, Phosphorus Sulfur Silicon Relat. Elem. 195 (2020) 779–804, https://doi.org/10.1080/10426507.2020.1764956.

[31] U. Solmaz, I. Gumus, G. Binzet, O. Celik, G.K. Balci, A. Dogen, H. Arslan, Synthesis, characterization, crystal structure, and antimicrobial studies of novel thiourea derivative ligands and their platinum complexes, J. Coord. Chem. 71 (2018) 200–218, https://doi.org/10.1080/00958972.2018.1427233.

[32] S. Adhikari, O. Hussain, R.M. Phillips, W. Kaminsky, M.R. Kollipara, Synthesis, structural and chemosensitivity studies of arene d^6 metal complexes having *N*-phenyl-*N'*-(pyridyl/pyrimidyl)thiourea derivatives, Appl. Organomet. Chem. 32 (2018) e4362.

[33] M. Kalidasan, R. Nagarajaprakash, K.M. Rao, Synthesis and molecular studies of half-sandwich arene ruthenium and Cp*Rh/Cp*Ir complexes containing (3-picolyl) thiourea derivatives as N, S-bidentate donor ligands, Transition Met. Chem. 40 (2015) 531–539, https://doi.org/10.1007/s11243-015-9946-x.

[34] S.I. Orysyk, V.V. Bon, V.I. Pekhnyo, Y.L. Zborovskii, V.V. Orysyk, M.V. Vovk, Synthesis, structure and spectral characteristics of Ni(II), Pd(II) and Zn(II) complexes with *N*-(2-pyridinyl)morpholine-4-carbothioamide, Polyhedron 38 (2012) 15–25, https://doi.org/10.1016/j.poly.2012.02.017.

[35] M.J.M. Campbell, Transition metal complexes of thiosemicarbazide and thiosemicarbazones, Coord. Chem. Rev. 15 (1975) 279–319, https://doi.org/10.1016/S0010-8545(00)80276-3.

[36] T.S. Lobana, R. Sharma, G. Bawa, S. Khana, Bonding and structure trends of thiosemicarbazone derivatives of metals–An overview, Coord. Chem. Rev. 253 (2009) 977–1055, https://doi.org/10.1016/j.ccr.2008.07.004.

[37] S.I. Orysyk, V.V. Bon, O.O. Zholob, V.I. Pekhnyo, V.V. Orysyk, Y.L. Zborovskii, M. V. Vovk, Novel Pd(II) coordination compounds involving 2-[(2-hydroxyphenyl) methylene]hydrazine-*N*-(2-propenyl)-carbothioamide as a ligand or proligand: Synthesis, crystal structures and analytical application, Polyhedron 51 (2013) 211–221, https://doi.org/10.1016/j.poly.2012.12.021.

[38] N.K. Hien, N.C. Bao, N.T.A. Nhung, N.T. Trung, P.C. Nam, T. Duong, J.S. Kim, D. T. Quang, A highly sensitive fluorescent chemosensor for simultaneous determination of Ag(I), Hg(II), and Cu(II) ions: Design, synthesis, characterization and application, Dyes Pigments 116 (2015) 89–96, https://doi.org/10.1016/j.dyepig.2015.01.014.

[39] S. Kuchekar, R. Naval, S.-H. Han, Development of a reliable method for the spectrophotometric determination of palladium(II) with o-methoxyphenyl thiourea: Separation of palladium from associated metal ions, S. Afr. J. Chem. 67 (2014) 226–232. https://hdl.handle.net/10520/EJC164273.

[40] (a) G. Marverti, M. Cusumano, A. Ligabue, M.L. Di Pietro, P.A. Vainiglia, A. Ferrari, M. Bergomi, M.S. Moruzzi, C. Frassineti, Studies on the anti-proliferative effects of novel DNA-Intercalating bipyridyl-thiourea-Pt(II) complexes against cisplatin-sensitive and -resistant human ovarian cancer cells, J. Inorg. Biochem. 102 (4) (2008) 699–712, https://doi.org/10.1016/j.jinorgbio.2007.10.015;
(b) Q. Zhou, C. You, Y. Ling, H. Wu, B. Sun, pH and thermo dual stimulus-responsive liposome nanoparticles for targeted delivery of platinum-acridine hybrid agent, Life Sci. 217 (2019) 41–48, https://doi.org/10.1016/j.lfs.2018.11.052.

[41] (a) M.K. Amir, Z. Khan, I. Ahmad, J.A. Nasir, S. Abbas, Z. Rehman, F. Ud Din, T. Kondratyuk, F. Ɓelanger-Gariepy, New [Pt(S2CNR2)Cl(PAr3)] complexes as anticancer agents, Inorg. Chem. Com. 136 (2022) 109142, https://doi.org/10.1016/j.inoche.2021.109142;
(b) ShZ. Khan, Z. Khan, I. Ahmad, S. Khan, S. Khan, M. Ahmed, M. Inam, F. Ɓelanger-Gariepy, Z. ur Rehman, Structural features, anticancer, antioxidant and anti-acetylcholinesterase studies of [(DTCs)(PAr3)PdCl], Inorg. Chem. Com. 123 (2021), https://doi.org/10.1016/j.inoche.2020.108316.

[42] H.H. Repich, V.V. Orysyk, L.G. Palchykovska, S.I. Orysyk, Y.L. Zborovskii, O. V. Vasylchenko, O.V. Storozhuk, A.A. Biluk, V.V. Nikulina, L.V. Garmanchuk, V. I. Pekhnyo, M.V. Vovk, Synthesis, spectral characterization of novel Pd(II), Pt(II) π-coordination compounds based on N-allylthioureas, Cytotoxic properties and DNA binding ability, J. Inorg. Biochem. 168 (2017) 98–106, https://doi.org/10.1016/j.jinorgbio.2016.12.004.

[43] S.I. Orysyk, P.V. Borovyk, H.H. Repich, O.V. Severynovska, Y.L. Zborovskii, A. M. Mishchenko, V.V. Orysyk, V.I. Pekhnyo, M.V. Vovk, Synthesis, spectral characterization and DFT calculations of novel Ag(I) π-coordination polymeric complexes based on N-allylmorpholine-4-carbothioamide, 127866, J. Mol. Struct. 1208 (2020), https://doi.org/10.1016/j.molstruc.2020.127866.

[44] S.I. Orysyk, S. Baranets, P.V. Borovyk, L.G. Palchykovska, Y.L. Zborovskii, V.V. Orysyk, A.F. Likhanov, M.O. Platonov, D.B. Kovalskyy, T.V. Shyryna, Y. Danylenko, V.V. Hurmach, V.I. Pekhnyo M.V. Vovk, Mononuclear π-complexes of Pd(II) and Pt(II) with 1-allyl-3-(2-hydroxyethyl)thiourea: Synthesis, structure, molecular docking, DNA binding ability and genotoxic activity, Polyhedron 210 (2021) 115477, 10.1016/j.poly.2021.115477.

[45] V.V. Bon, S.I. Orysyk, V.I. Pekhnyo, V.V. Orysyk, S.V. Volkov, Synthesis and spectroscopic investigations of Rh(III) and Pd(II) complex compounds with N-(pyridine-2-yl)-morpholine-4-carbothioamide, Polyhedron 26 (2007) 2935–2941, https://doi.org/10.1016/j.poly.2007.01.042.

[46] S.I. Orysyk, V.V. Bon, V.I. Pekhnyo, *cis-bis*[1-allyl-3-(2-pyridyl-κN)thioureato-κS] palladium(II), Acta Cryst. E65 (2009), m1059, https://doi.org/10.1107/S1600536809029262.

[47] S. Orysyk, V. Pekhnyo, V. Orysyk, Yu. Zborovskii, P. Borovyk, M. Vovk, Fundamental aspects of the coordination chemistry of transition metals with functionaly substotuted thioamides (Part I), Ukr. Chem. Journ. 88(2) (2022) 85–115, 10.33609/2708-129X.88.02.2022.85-115. b) S. Orysyk, V. Pekhnyo, V. Orysyk, Yu. Zborovskii, P. Borovyk, M. Vovk, Fundamental aspects of the coordination chemistry of transition metals with functionaly substotuted thioamides (Part II), Ukr. Chem. Journ. 88(3) (2022) 3–27, 10.33609/2708-129X.88.03.2022.3-27.

[48] P.V. Borovyk, S.I. Orysyk, H.H. Repich, A.F. Likhanov, A.M. Mishchenko, Yu.L. Zborovskii, V.V. Orysyk, L.G. Palchikovska, V.I. Pekhnyo, M.V. Vovk, Spectral characteristics and cytostatic effect of Pd(II) and Pt(II) carbothioamide π-complexes on *Allium cepa* L meristem cells, Voprosy khimii i khimicheskoi tekhnologii. 3 (2020) 34-45, 10.32434/0321-4095-2020-130-3-34-45.

[49] R.G. Pearson, Antisymbiosis and the trans effect, Inorg. Chem. 12 (1973) 712–713, https://doi.org/10.1021/ic50121a052.

[50] J.D. Roberts, M.C. Caserio, Basic principles of organic chemistry, 2022, LibreTexts Project, https://LibreTexts.org.

[51] E. Pretsch, Ph Buhlmann, M. Badertscher, Structure Determination Of Organic Compounds. Tables of Spectral Data, Springer-Verlag Berlin Heidelberg, 2009, 10.1007/978-3-540-93810-1.

[52] G. Socrates, Infrared and Raman Characteristic Group Frequencies. Tables and Charts, Third ed., by John Wiley & Sons Ltd, 2001, p. 347.

[53] B. Smith, Infrared spectral interpretation: a systematic approach, 2000 N.W., 265 p.

[54] V. Ţucureanu, A. Matei, A. Marius Avram, FTIR spectroscopy for carbon family study, Crit. Rev. Anal. Chem. 46 (6) (2016) 502–520, https://doi.org/10.1080/10408347.2016.1157013.

[55] A.B.P. Lever, Inorganic Electronic Spectroscopy, Toronto, Canada, American Elsevier Publishing Co., New York, 1968, p. 420.

[56] E. Viola, et al., Synthesis and structure of rare zwitterionic complexes involving the presence of $N_{(py)}MCl_3^-$ moieties (M = Pt(II), Pd(II)), Inorg. Chim. Acta 480 (2018) 101–107.

[57] O.-E. Schultz, K. Gleixner, Transportformen von Isothiocyanaten, Stabilitat und Spaltbarkeit, Arch. Pharmaz. 295 (1962) 879–894, https://doi.org/10.1002/ardp.19622951204.

[58] L. Novák, M. Hanania, P. Kovács, C.E. Kovács, P. Kolonits, C. Szántay, A convenient route to cyanoguanidines, Synth. Commun. 29 (1999) 1757–1766, https://doi.org/10.1080/00397919908086163.

[59] G.M. Sheldrick, Acta Cryst. A 64 (2008) 112–122, https://doi.org/10.1107/S0108767307043930.

[60] L. Garmanchuk, O.M. Perepelytsina, M.V. Sidorenko, L.I. Ostapchenko, Growth kinetics of 2- and 3-D cell models as influenced by the microenviroment, Cytology and genetics 43 (2009), p305, https://doi.org/10.3103/S0095452709050028.

[61] T.V. Nikolaienko, L.V. Garmanchuk, Y.A. Stupak, Effective model for antitumor drugs screening based on 3D growth system of MCF-7, Annals of Oncology 29 (2018), https://doi.org/10.1093/annonc/mdy047.047.

[62] J.D. Dunitz, H.-B. Bürgi (Eds.), Structure Correlation, VCH Verlagsgesellschaft mbH, Weinheim, 1994.

[63] M.D. Hall, K.A. Telma, K.-E. Chang, T.D. Lee, J.P. Madigan, J.R. Lloyd, I. S. Goldlust, J.D. Hoeschele, M.M. Gottesman, Say no to DMSO: dimethylsulfoxide inactivates cisplatin, carboplatin, and other platinum complexes. Say no to DMSO: dimethylsulfoxide inactivates cisplatin, carboplatin, and other platinum complexes, Cancer Res. 74 (2014) 3913–3922, https://doi.org/10.1158/0008-5472.CAN-14-0247.

[64] L. Kelland, The resurgence of platinum-based cancer chemotherapy, Nat. Rev. Cancer 7 (2007) 573–584, https://doi.org/10.1038/nrc2167.

[65] L. Pulze, T. Congiu, T.A.L. Brevini, A. Grimaldi, G. Tettamanti, P. D'Antona, N. Baranzini, F. Acquati, F. Ferraro, M. de Eguileor, MCF7 spheroid development: new insight about spatio/temporal arrangements of TNTs, amyloid fibrils, cell connections and cellular bridges, Int. J. Mol. Sci. 21 (2020) 5400, https://doi.org/10.3390/ijms21155400.

[66] C.J. Lovitt, T.B. Shelper, V.M. Avery, Miniaturized three-dimensional cancer model for drug evaluation, Assay Drug Dev. Technol. 11 (7) (2013) 435–448, https://doi.org/10.1089/adt.2012.483.

[67] G. Lazzari, P. Couvreur, S. Mura, Multicellular tumor spheroids: a relevant 3D model for the in vitro preclinical investigation of polymer nanomedicines, Polymer Chem. 8 (2017) 4947–4969, https://doi.org/10.1039/C7PY00559H.

[68] K. Ono, K. Sato, T. Nakamura, Y. Yoshida, S. Murata, K. Yoshida, H. Kanemoto, K. Umemori, H. Kawai, K. Obata, S. Ryumon, K. Hasegawa, Y. Kunisada, T. Okui, S. Ibaragi, H. Nagatsuka, A. Sasaki, Reproduction of the antitumor effect of cisplatin and cetuximab using a three-dimensional spheroid model in oral cancer, Int. J. Med. Sci. 19 (8) (2022) 1320–1333, https://doi.org/10.7150/ijms.74109.